Ineluctability of Oscillations in Systems With Digital Implementation of Derivative Feedback

Andrew H. C. Gosline [a], Vincent Hayward [b], Hannah Michalska [c]

[a] *Children's Hospital Boston, Harvard Medical School, Boston,* USA

[b] UPMC *Univ Paris 06, Institut des Systèmes Intelligents et de Robotique, Paris, France*

[c] *Department of Electrical and Computer Engineering, McGill University, Montréal, Qc, Canada*

Abstract

Differentiation in the feedback is common practice in digital control. Yet, the fundamental behavior of the universally employed backward difference of quantized signals has not been studied thus far. We show that velocity always oscillates when this type of feedback is applied to a forced, linear second-order system for any system parameter. We then compute a bound for the oscillation amplitude which can be easily computed given the parameters of the system. Experimental results are in close agreement with the theory. If the system has dry friction, our study yields a sufficient condition for the quenching of spontaneous oscillations.

Key words: Digital control systems, quantization and sampling, velocity estimation.

1 Introduction

Numerous control systems rely on the numerical differentiation of the output measurement in order to provide feedback. Most commonly, these control systems employ proportional-integral-derivative (PID) control. In continuous time, it is immediate from Fig. 1 that the measurement noise, w, injected in the loop is amplified by differentiation. Actual implementations remedy this problem by augmenting strict differentiation with various filters that attenuate high frequency noise. There are many types, and names, of such filters ("dirty derivative", "approximate derivative", "band limited derivative", and so on), all causing phase lag.

Digitally-realized PID control, [14], is also affected by noise and time delays whose occurrence is inherent in numerical differentiation. Quantization error, often modeled as noise, which accompanies any numerical implementation, is unavoidable. Even if the effects of analog noise can be neglected, as with digital shaft encoders, or when the analog noise is smaller than the quantization step of a converter, the quantization noise should not be neglected.

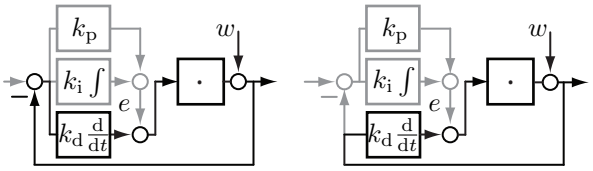

Fig. 1. Block diagrams of common types of PID control showing how noise, w, is injected into the control loop via a signal path shown in black.

So severe is this problem that despite the continuing importance of PID control—not fewer than 56 patents on this topic have been granted worldwide between 1990 and 2000—, in actual practice 80% of PID controllers have the derivative part omitted or switched off [2].

Other applications in which differentiation of the output measurement is necessary include virtual reality systems with haptic feedback. Such systems typically involve an electromechanical device that responds to torque commands with the objective to modify the dynamics of the device to simulate the stiffness and viscosity of virtual objects. The required modification is typically accomplished by feeding back suitably processed quantized position measurements as torque inputs.

Email addresses:
andrew.gosline@childrens.harvard.edu (Andrew H. C. Gosline), vincent.hayward@isir.upmc.fr (Vincent Hayward), hannah.michalska@mcgill.ca (Hannah Michalska).

Figure 2 shows the minimum digital implementation of the simulation of viscosity. A more detailed description of the signals appearing in the figure is delayed until Section 2. Referring to the signal path (in black) of Fig. 1, notice that the zero-order-hold (ZOH) sampling of the derivative feedback loop of the PID would be identical.

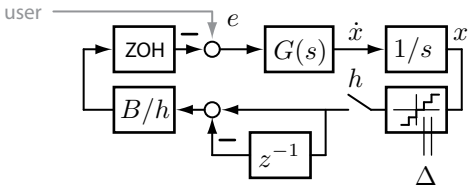

Fig. 2. Block Diagram of simulation of viscosity B at sampling period h. Signal e represents a forcing input to the system due to the user's hand.

Quantizers are nonlinear elements that can be represented by several basic models according to implementation. Incremental encoders modify the content of a pulse counter which is read at the instants of sampling. Hysteresis may have to be accounted for because after a velocity reversal the same incremental position corresponds to counts that differ by one unit. However, modern circuits have a feature that suppresses the first count after a reversal, eliminating hysteresis. In the latter case, the single-valued floor function represents incremental encoder quantization. For devices having analog sensors and analog-to-digital converters, quantization can, in certain cases, be better represented by the rounding function whose value is obtained by adding $\frac{1}{2}$ to the argument variable, before application of the floor operation. In other cases, $\frac{1}{2}$ must be added *after* application of the floor operation. The results of this paper are not affected by these distinctions since only increments of quantized values are considered. In other circumstances, however, these distinctions are important [19].

The output signal of the system shown in Fig. 3 makes it apparent that the backward difference of quantized signals exhibits a peculiar nonlinear behavior giving a choppy output even if a smooth, noise-free input is used. It is also important to note that the velocity estimation oscillates according to the fundamental velocity quantum of $\nu \triangleq \Delta/h$ that is nothing else but the Courant-Friedrichs-Lewy critical velocity that participates in the stability of systems quantized in time and space [20]. The noise has a wide and time-varying spectrum that precludes devising simple design rules for smoothing filters.

To attenuate quantization error, the use of the inverse-time method [23,17,16], adaptive FIR filters [12], Kalman filtering [3], or else observers such as that in [21,22] have been advocated both for control purposes and for virtual reality applications. All of these methods involve tradeoffs. Inverse time methods require special hardware, introduce variable time delay, fail to account for rapid signal variations, and break down at high velocities. Adaptive filters address these problems better but require tuning. The Kalman filter and observer approaches are slow in response or must rely on accurate models of the system and of disturbances which are rarely available.

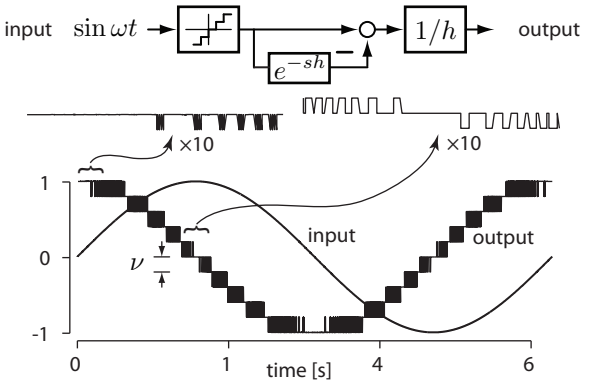

Fig. 3. Effects of backward difference of quantized sinusoidal signal. Here, $\Delta = 0.002$, $h = 0.01$, $\omega = 2\pi$, and $\nu = 0.2$.

The need to compensate for quantization noise is not restricted to electromechanical systems. It arises whenever the time derivative of a state must be estimated from measurements. Regarding the generality and importance of the problem, the question of the effect of quantization on discrete differentiation has been mentioned as early as in [24], where it was noted that it could induce oscillations in feedback systems. Rigorous analysis of the phenomenon has so far been addressed mostly via stochastic approaches [10,13].

Many previous results pertaining to the behavior of closed-loop quantized systems are available, addressing mostly the question of stabilization [7,18,15] or channel rate, see [11], for a rcent survey, but these works do not address explicitly the problems due to differentiation of quantized signals in the feedback.

Motivated by this discussion, the aim of this paper is to rigorously address the essence of the problem of oscillations inherent in digital control systems. Since complex system dynamics is often well approximated in terms of the dynamics associated with the dominant poles, the oscillatory behavior of digital systems is analyzed here while employing the simplest meaningful model—a linear second order system with feedback involving digital differentiation. Nonlinear and higher order models have not yet been studied under similar conditions as the analysis of these models are likely to involve complex phenomena such as chaos.

The fundamental behavior of the universally employed backward difference of quantized signals in feedback to a forced second-order system is hence studied as depicted in the diagram of Fig. 2, where $G(s)$ represents the first order lag,

$$G(s) = \frac{1}{ms + b}.$$

The system considered is not merely an idealization but actually happens to coincide with many electromechanical systems with PID control or with the virtual reality systems alluded to.

It is shown that such forced second-order system including a feedback loop with discrete differentiation of a quantized output fails to reach a steady-state, while producing sustained oscillations. These oscillations exist for *any value* of the system parameters unless the forcing input is zero. Unlike position feedback, where the effects of delay and quantization can be eliminated if viscosity is sufficiently high, or if the sampling period is sufficiently short [6,1,8], the oscillatory effects of quantized differentiation cannot be eliminated by increasing viscosity.

They can be reduced, however, and a bound for the oscillation amplitude can be expressed in terms of the parameters of the continuous system: the sampling period, the size of the quantization step, and the magnitude of the forcing input.

The results are validated by means of an experimental setup in the area of haptic rendering where all the relevant parameters can be continuously adjusted by varying viscosity. The results obtained in the experiments are in agreement with numerical simulations and remain in close agreement with the theoretical bound.

2 Genesis of Oscillations Rooted in the Lack of Steady-State

Employing the simplest example of a digitally controlled system, as in the diagram in Fig. 2, it will be shown that the essence of the problem of persistent oscillations lies in the absence of a well-defined steady state. More precisely, it will be shown that in the absence of external noise and under constant forcing signals, the set of system parameters for which the system possesses a steady state velocity is of measure zero. External disturbances being unavoidable, the system velocity cannot converge to any steady state even if it is stable, exhibiting some pattern of oscillatory behavior.

Let h represent the sampling period, Δ the quantization step, and x the measured output. Notice that in the aforementioned two cases, a velocity loop is forced by an exogenous, slow-varying signal, e, arising from the proportional-integral feedback and in virtual reality from the force applied by the user's hand. A signal, $x(t)$, sampled at time $t = kh$ is noted x_k. For convenience, let $\sigma = x/\Delta$ be the displacement normalized to the quantizer resolution. The diagram shown in Fig. 2 represents the following system:

$$m\ddot{x}(t) + b\dot{x}(t) = e(t) - B\nu\left(\lfloor\sigma_k\rfloor - \lfloor\sigma_{k-1}\rfloor + \varepsilon(t)\right), \quad (1)$$

$\forall k \in \mathbb{N}, t \in [kh, (k+1)h)$, where $\lfloor\cdot\rfloor$ stands for the standard floor operator returning the smallest integer value not exceeding the value of its argument, and $\varepsilon(t)$ represents analog noise.

Remark 1 *System* (1) *represents a hybrid, discrete and continuous time nonlinear system with time delay, and as such, does not lend itself to immediate assessment with regard to its qualitative and quantitative behavior. One could represent the output,* $\lfloor x(t)\rfloor$*, by* $x(t) + q(t)$*, with* $x(t)$ *denoting the continuous-time input to the quantizer and* $q(t)$ *the discontinuous quantization error. With this substitution,* (1) *is 'transformed' into a sampled-data linear system with two inputs,* $e(t)$ *and* $q(t)$*. However appealing is the substitution, it does not represent a standard sampled-data system since* $q(t)$ *is not exogenous. It is a function of the parameters, of the sampling interval, and of initial conditions. For this reason, stochastic and frequency domain approaches are unable to precisely address the question of oscillations since such approaches effectively omit the feedback that links* $x(t)$ *to the error in the system velocity estimate.*

First consider a restricted noise-free system (1) forced by a constant, non-zero input e, written in the form

$$\begin{aligned} \dot{x}(t) &= v(t), \\ m\,\dot{v}(t) + b\,v(t) &= e - B\nu\left(\lfloor\sigma_k\rfloor - \lfloor\sigma_{k-1}\rfloor\right), \end{aligned} \quad (2)$$

$\forall k \in \mathbb{N}, t \in [kh, (k+1)h)$, with any given initial conditions $x(0) = x_0$, $v(0) = v_0$, while assuming that the unforced system $m\dot{v}(t) + bv(t) = 0$ is stable. The analog counterpart of this system is given by $\dot{x}(t) = v(t); m\dot{v}(t) + (b+B)v(t) = e$ with velocity response $v(t) = v_0 e^{-\alpha t} + v_\infty[1 - e^{-\alpha}]$, where $v_\infty = e/(b+B)$ represents the steady-state of the velocity subsystem and $\alpha \triangleq (b+B)/m$. Neglecting the transients, the position varies as a linear function of time $x(t) = x_0 + v_\infty t$. By analogy, the digitally implemented system is said to possess a steady-state velocity, v_∞, if the position function $x(t) = x_0 + v_\infty t, t \geq 0$, satisfies (2).

The parameters in (1) are not restricted in any way, the poles of the system are arbitrary provided that the unforced system is stable.

Theorem 1 (Existence of a steady state) *For system (2), with stable unforced system* $m\dot{v}(t) + bv(t) = 0$*, there exists a steady-state velocity if and only if*

$$\frac{e}{\nu(b+B)} \in \mathbb{N}. \quad (3)$$

If this condition is satisfied, the steady-state velocity is

$$v_\infty = e/(b+B). \quad (4)$$

Remark 2 *Following Remark 1 the proof must be carried out in the time domain and Condition* (3) *must be necessary and sufficient to ensure that the errors incurred*

by quantization of the state at two succeeding sampling instants $k-1$ and k produce a constant error in the velocity estimate. Any noise or inaccuracy in a practical implementation will cause (3) *to fail, compelling the system to oscillate since the set of steady state velocities is of measure zero.*

Proof. Suppose that Condition (3) holds. Then v_∞ given by (4) satisfies $v_\infty/\nu \in \mathbb{N}$. Let $x(\cdot)$ satisfy $\dot{x}(t) = v_\infty$, so $x_k = x_0 + v_\infty kh$, $k \in \mathbb{N}$. Then, $\forall k \in \mathbb{N}$,

$$\begin{aligned}\lfloor \sigma_k \rfloor - \lfloor \sigma_{k-1} \rfloor &= \left\lfloor \sigma_0 + \frac{v_\infty}{\nu} k \right\rfloor - \left\lfloor \sigma_0 + \frac{v_\infty}{\nu}(k-1) \right\rfloor \\ &= \lfloor \sigma_0 \rfloor - \lfloor \sigma_0 \rfloor + \frac{v_\infty}{\nu} = \frac{v_\infty}{\nu}, \end{aligned} \tag{5}$$

since for any numbers $a \in \mathbb{R}$, $i \in \mathbb{N}$, $\lfloor a + i \rfloor = \lfloor a \rfloor + i$. Consequently, if v_∞ is given by (4) then $x(t) = x_0 + v_\infty t$, satisfies (2) confirming that v_∞ is indeed the steady state velocity of the system.

We now demonstrate that any error in the satisfaction of Condition (3) precludes the existence of a steady state velocity. Call $D_k \triangleq \{d_k\}_{k\in\mathbb{N}}$ the integer sequence such that

$$d_k = \lfloor \sigma_k \rfloor - \lfloor \sigma_{k-1} \rfloor, \quad \forall k \in \mathbb{N}. \tag{6}$$

Suppose that (3) does not hold but that some v_0 is a steady state velocity for the system. By definition, $x(t) = x_0 - v_0 t$ satisfies (2) requiring that the sequence D_k is constant with terms d_k satisfying $\forall k \in \mathbb{N}$,

$$d_k = \frac{e - bv_0}{B\,\nu} = \left\lfloor \sigma_0 + \frac{v_0}{\nu} k \right\rfloor - \left\lfloor \sigma_0 + \frac{v_0}{\nu}(k-1) \right\rfloor. \tag{7}$$

If $v_0/\nu \in \mathbb{N}$ then a calculation identical to that in (5) would show that $d_k = (e - bv_0)/(B\,\nu) = v_0/\nu$ implying that $v_0 = v_\infty$ and the validity of Condition (3), which is a contradiction. Hence v_0 is not a multiple of ν, and without the loss of generality, x_0 is not a multiple of Δ (for if not then one could consider $x(t)$ to defined on some restricted interval of time $[t', +\infty), t' > 0$.) Then $x_0 = \Delta(k_1 + \epsilon_1)$ and $v_0 = \nu(k_2 + \epsilon_2)$, with k_1, $k_2 \in \mathbb{N}$ and ϵ_1, $\epsilon_2 \in [0, 1)$. Noting that $\epsilon_2 > 0$, $\forall k \in \mathbb{N}$,

$$\begin{aligned} d_k &= \lfloor k_1 + \epsilon_1 + kk_2 + k\epsilon_2 \rfloor - \\ &\qquad \lfloor k_1 + \epsilon_1 + (k-1)k_2 + (k-1)\epsilon_2 \rfloor \\ &= k_2 + \lfloor \epsilon_1 + k\epsilon_2 \rfloor - \lfloor \epsilon_1 + (k-1)\epsilon_2 \rfloor. \end{aligned}$$

Suppose first that $\epsilon_1 + \epsilon_2 < 1$. Then,

$$d_1 = k_2 + \lfloor \epsilon_1 + \epsilon_2 \rfloor - \lfloor \epsilon_1 \rfloor = k_2. \tag{8}$$

Let k to be the smallest integer such that $\epsilon_1 + k\epsilon_2 \geq 1$. Then,

$$\begin{aligned} d_k &= k_2 + \lfloor \epsilon_1 + k\epsilon_2 \rfloor - \lfloor \epsilon_1 + (k-1)\epsilon_2 \rfloor \\ &= k_2 + 1 - 0 = k_2 + 1. \end{aligned} \tag{9}$$

Equations (8) and (9) imply that D_k is not a constant sequence. Suppose now that $\epsilon_1 + \epsilon_2 \geq 1$ and let n be the smallest natural number such that,

$$\epsilon_1 + n(\epsilon_2 - 1) + \epsilon_2 < 1. \tag{10}$$

Such a natural number exists because $\epsilon_2 - 1 < 0$. It follows that

$$\begin{aligned} &\epsilon_1 + (n-1)(\epsilon_2 - 1) + \epsilon_2 \geq 1 \\ &\quad \Rightarrow \epsilon_1 + (n-1)\epsilon_2 + \epsilon_2 - (n-1) \geq 1 \\ &\quad \Rightarrow \epsilon_1 + n(\epsilon_2 - 1) \geq 0. \end{aligned}$$

Defining $\epsilon_1' \triangleq \epsilon_1 + n(\epsilon_2 - 1)$, implies

$$\epsilon_1' + \epsilon_2 = \epsilon_1 + n(\epsilon_2 - 1) + \epsilon_2 < 1.$$

Then, consider a new shifted sequence $D_k' = \{d_k'\}$, $k \in \mathbb{N}$ defined in terms of ϵ_1' such that

$$\begin{aligned} d_k' &= k_2 + \lfloor \epsilon_1' + k\epsilon_2 \rfloor - \lfloor \epsilon_1' + (k-1)\epsilon_2 \rfloor \\ &= k_2 + \lfloor \epsilon_1 + n(\epsilon_2 - 1) + k\varepsilon_2 \rfloor \\ &\qquad - \lfloor \epsilon_1 + n(\epsilon_2 - 1) + (k-1)\epsilon_2 \rfloor \\ &= k_2 + \lfloor \epsilon_1 + n\epsilon_2 + k\epsilon_2 \rfloor - \lfloor \epsilon_1 + n\epsilon_2 + (k-1)\epsilon_2 \rfloor \\ &= k_2 + \lfloor \epsilon_1 + (n+k)\epsilon_2 \rfloor - \lfloor \epsilon_1 + (n+k-1)\epsilon_2 \rfloor \\ &= d_{n+k}. \end{aligned}$$

Then,

$$d_{n+1} = d_1' = k_2 + \lfloor \epsilon_1' + \epsilon_2 \rfloor - \lfloor \epsilon_1' \rfloor = k_2. \tag{11}$$

Similarly, let l be the smallest integer that is such that $\epsilon_1' + l\epsilon_2 \geq 1$. It follows that

$$\begin{aligned} d_{n+l} = d_l' &= k_2 + \lfloor \epsilon_1' + l\epsilon_2 \rfloor - \lfloor \epsilon_1' + (l-1)\epsilon_2 \rfloor \\ &= k_2 + 1 + 0 = k_2 + 1. \end{aligned} \tag{12}$$

Again, (11) and (12) imply that D_k is not a constant sequence. This completes the proof. □

Remark 3 *The introduction of digital position or digital integration terms in the system feedback do not change the "non-robust" nature of the system steady-state. To see this, suppose that the second order system is controlled by full digital* PID *compensation:*

$$\begin{aligned} m\ddot{x}(t) + b\dot{x}(t) &= k_\mathrm{p}\, h\nu \left(\lfloor \sigma_{\mathrm{d}_k} \rfloor - \lfloor \sigma_k \rfloor \right) \\ &\quad + k_\mathrm{i}\, h\nu \sum_{i=0}^{k} \left(\lfloor \sigma_{\mathrm{d}_k} \rfloor - \lfloor \sigma_i \rfloor \right) \\ &\quad - k_\mathrm{d} \nu \left(\lfloor \sigma_k \rfloor - \lfloor \sigma_{k-1} \rfloor \right), \end{aligned} \tag{13}$$

$\forall k \in \mathbb{N}, t \in [kh, (k+1)h)$, *where* σ_d *is the desired normalized system state. First let* $k_\mathrm{i} = 0$. *If* v_∞ *is some non-zero steady-state velocity of the system then the sequence of samples associated with position would diverge*

as $||\lfloor \sigma_k \rfloor|| = ||\lfloor \sigma_0 + v_\infty/\nu k \rfloor|| \to \infty$ *with* $k \to \infty$ *unless* $v_\infty = 0$. *The sequence of digital estimates of the velocity,* $D_k = \{\lfloor\sigma_k\rfloor - \lfloor\sigma_{k-1}\rfloor\}_{k\in\mathbb{N}}$, *however, would remain bounded. Hence, the* RHS *of* (13) *could only be zero if* $v_\infty = 0$. *The corresponding steady state position would then be any* x_∞ *such that* $\lfloor\sigma_\infty\rfloor = \lfloor\sigma_\mathrm{d}\rfloor$. *It is not reasonable to expect that* $D_k = \{0\}_{k\in\mathbb{N}}$ *exactly, so oscillations would be imminent. With an integral term,* $k_\mathrm{i} \neq 0$, v_∞ *would similarly have to be zero, implying that the quantized position would have to satisfy* $k_\mathrm{p} h\nu\,(\lfloor\sigma_\mathrm{d}\rfloor - \lfloor\sigma_\infty\rfloor) + k_\mathrm{i} h(k+1)\,(\lfloor\sigma_\mathrm{d}\rfloor - \lfloor\sigma_\infty\rfloor) = 0, k \in \mathbb{N}$, *hence implying the absence of steady-state regulation error with the precision of quantization, that is* $\lfloor\sigma_\mathrm{ss}\rfloor = \lfloor\sigma_\mathrm{d}\rfloor$. *Similarly, oscillations would arise from any deviation from the condition* $D_k = \{0\}_{k\in\mathbb{N}}$.

3 Boundedness of Oscillations

Conditions for BIBO stability of the system depicted by Fig. 2 can be derived to yield an explicit bound for the oscillations. The derivation is, again, performed in the time domain since a frequency-domain approach would neglects the internal coupling between the quantization error and the system dynamics. A time-domain evaluation based on summation of a von Neumann series delivers a more precise bound than the Parseval's equality.

Let l_∞, l_1 denote the spaces of bounded real sequences $X \triangleq \{x_k\}_{k\in\mathbb{N}}$ such that $\|X\|_\infty \triangleq \sup_{k\in\mathbb{N}}|x_k| < \infty$ and $\|X\|_1 \triangleq \sum_{k\in\mathbb{N}}|x_k| < \infty$, respectively, let $L_\infty[0,\infty)$ denote the space of all essentially bounded, Lebesgue integrable, real functions $f : [0,\infty) \to \mathbb{R}$ such that $\|f\|_\infty \triangleq \operatorname{ess\,sup}_{t\in[0,\infty)}|f(t)| < \infty$, and consider the natural discretization of system (2) with time step h. In the foregoing let $\{\eta_l\}_{l=0}^\infty$ be the sequence of discretization errors, $\eta_l \triangleq \lfloor\sigma_l\rfloor - \sigma_l$, $\forall l \in \mathbb{N}$. Recall that the uncontrolled system has a damping coefficient b which is to be augmented by B. Call $\tau_n = m/b$ and $\tau_b = m/B$ the natural and artificial time constants, respectively. Let $\alpha(t) \triangleq \exp(-(t-kh)/\tau_n)$ be the free response at step k and $\alpha_h = \exp(-h/\tau_n)$ be the response after one sampling period. It is convenient to introduce $\kappa = B/b$, the proportion of artificial to natural damping, $\rho = 1/\Delta$, and $\xi = 1/h$, the quantizer spatial frequency and the sampling frequency, respectively. Recall that $\nu = \Delta/h$ is the critical velocity quantum.

Theorem 2 (Boundedness) *The noise-free system* (2) *is* L_∞-BIBO *stable if*

$$r(\Phi) \triangleq \max_{i=1,2}\{|\lambda_i(\Phi)|\} < 1. \tag{14}$$

For a constant forcing input e, *the velocity output defined as the sequence* $\{v_k\}_{k\in\mathbb{N}}$ *is asymptotically bounded,*

$$\|\{v_k\}_{k\in\mathbb{N}}\|_\infty \le |e|\,\left|C(I-\Phi)^{-1}\Gamma_1\right| + \|\{\eta_{l+1}-\eta_l\}_{l=0}^\infty\|_\infty \left\|\{C\Phi^l\Gamma_2\}_{l=0}^\infty\right\|_1 + O(k),$$ *where*

$$\Phi = \begin{pmatrix} -\kappa\,(1-\xi\tau_n(1-\alpha_h)) & \rho\tau_n(1-\alpha_h) \\ -\kappa\nu(1-\alpha_h) & \alpha_h \end{pmatrix},$$

$$\Gamma_1 = \begin{pmatrix} \nu/b\,(1-\xi\tau_n(1-\alpha_h)) \\ 1/b(1-\alpha_h) \end{pmatrix},$$

$$\Gamma_2 = \begin{pmatrix} \kappa\,(1-\xi\tau_n(1-\alpha_h)) \\ \kappa\nu(1-\alpha_h) \end{pmatrix}, \quad C = [0\ 1].$$

Moreover, Condition (14) *is also necessary whenever* $[\Phi, \Gamma_1]$ *is controllable, that is when the natural discretization of the system is non-pathological.*

A shortened proof is delegated to the Appendix as it is straightforward.

4 Experimental Validation

To investigate the validity of the results of Theorems 1 and 2, experiments were completed with both numerical simulations and a physical apparatus.

4.1 Apparatus

Figure 4 shows a machine that was built to be modeled by (1). Two high-quality DC motors (model RE25-118751, Maxon Motors AG) are mounted co-axially and coupled together. Each motor is driven with a separate current amplifier (model LCAM, Quanser Consulting, Markam, ON, CA). One of the motors represents e, a slowly varying force. The second motor receives feedback via B. To modify conveniently the system parameters, an eddy-current damper is also mounted co-axially with the two motors. Such dampers are capable of precise and adjustable production of pure viscosity [9] and permitted to adjust the system's natural time constant, τ_n, over a wide range of values. An optical encoder (model R119, Gurley Precision Instruments, Troy, NY, USA) monitors the rotation of the common axis.

The damping coefficient, b, was calibrated from the steady-state velocity when giving a constant torque input. Damping coefficients for each coil current were recorded and averaged. The calibration was accurate to approximately 5%. The inertia, m, was fine-tuned by matching the first order response to a step input. The high resolution encoders, having 2^{16} counts per revolution, can resolve 9.59×10^{-5} rad. In order to observe the oscillations due to quantization with a single sensor, the software was set to decimate pulses by a factor 1 000

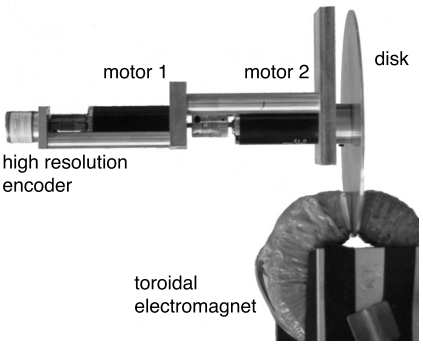

Fig. 4. Experimental Apparatus. Two parallel coupled torquers with an eddy current damper.

to mimic lower resolutions, while recording the trajectories at full resolution, causing the effective resolution to be 0.096 rad.

4.2 Results

Theorem 2 predicts that the oscillations of the system are bounded if and only if $\lambda(\Phi) \leq 1$. Taking $b = 1.26$ mN·m·s, m=0.14 g·m^2, $e = 50.0$ g·m^2, the system matrix was such that $\lambda(\Phi)$ was 0.9 or 1.1, by setting $h = 0.10$ and 0.15 s, or $B = 4.0$ and 5.5 mN·m·s, respectively. Figure 5 shows the results in the two cases. The simulation and the experimental results show that stability is well predicted despite some uncertainty in the system parameters. When the system is stable, in simulation like in experiments, oscillations diminish until they reach a sustained regime. When the system is unstable, the experimental oscillations grow until saturation, and the simulated oscillations grow indefinitely.

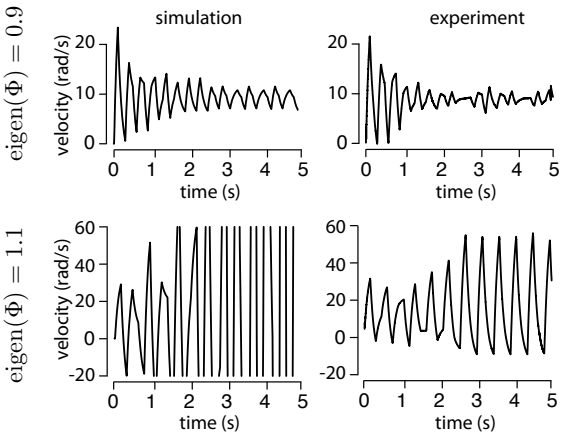

Fig. 5. System stability in two conditions where the system eigenvalues are smaller and larger than one.

Theorem 1 shows that a steady state velocity exists if and only if the steady-state velocity lies exactly on a velocity quantum. Velocity quanta are fixed by the sensor resolution and the sampling period, but the steady state velocity is related to the physical and virtual damping characteristics. Tiny variations in the physical damping coefficient prevented a steady state velocity from ever being reached. Experimental and simulation results agree with this finding, in that it was impossible to find parameters values where oscillations did not exist.

Table 1
Parameters used in Fig. 6.

		cases		
		(a)	(b)	(c)
b	[mN·m·s]	7.4	1.26	7.4
B	[mN·m·s]	3.0	2.0	11.0
v_∞	[rad/s]	4.7	15.0	2.7
nearest quanta	[rad/s]	3.9,4.8	14.5,15.5	1.9,3.8

Using the same m, Δ, and e as in the previous experiment, and $h = 0.1$ s, Figure 6 shows the results obtained with the three sets of parameters as per Table 1. Figure 6(a) shows the case where v_∞ is close to a velocity quantum: the oscillations are intermittent but persist. In Fig. 6(b) v_∞ is between two quanta: the oscillations are frequent. Figure 6(c) shows an example where the system flips between two different oscillation magnitudes. It is important to note that the simulated case was extremely sensitive to variations in the parameters of B or b. To achieve a good match between the simulation and the experiment b were tuned by approximately 5%, which is within the experimental error.

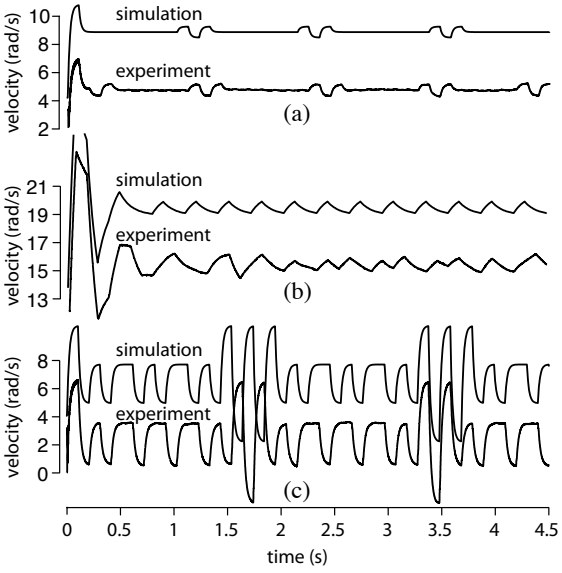

Fig. 6. Three specific cases of oscillations with parameters as per Table 2. To prevent the plots to fall on top of each other, the simulation plot was shifted upward. (a) Intermittent oscillations. (b) Frequent oscillations. (c) Complex oscillations.

The bounds established by Theorem 2 can be compared in simulation and in experiments. Table 2 collects the results. It is clear that the theoretical bound does indeed bound the maximum oscillation velocity when the initial

transients have vanished. It is also clear that the bound can be loose depending on the conditioning of the system. For example, the conditioning for Fig. 6(c) yields a maximum eigenvalue that is very close to 1, so the bound considerably overestimates the maximum velocity in stable oscillation because the geometric sequence from (25) is slow to converge.

Table 2
Comparaison between prediction and experiments.

		cases		
		(a)	(b)	(c)
		intermittent	frequent	complex
theoretical bound	[rad/s]	5.78	18.65	98.6
simulation	[rad/s]	5.06	15.6	6.60
experiment	[rad/s]	5.15	15.7	6.80
$\max(\lambda_i(\Phi))$	–	0.27	0.64	0.92
$\text{cond}(\Phi)$	–	3.80	4.11	35.7

5 Conclusion

Anyone who has tuned PID digitally-implemented controllers in the laboratory or in the field remembers having heard screeching or rumbling noises arising from the step-up when the D-gain is accidentally set too high; often at values considerably lower than those suggested by computer-aided tuning. The theory developed in this paper is an attempt to explain this phenomenon. It shows that oscillations are not only possible, but are in essence unavoidable. The theory that we developed allowed us to develop a bound for the magnitude of these oscillations that is entirely expressed in terms of system parameters. Simulations and experiments showed that this bound is an accurate predictor of actual oscillations that can exhibit an extraordinary variety of patterns; although these oscillations appear to be periodic in the deterministic case (see Fig. 7 for some other simulated examples).

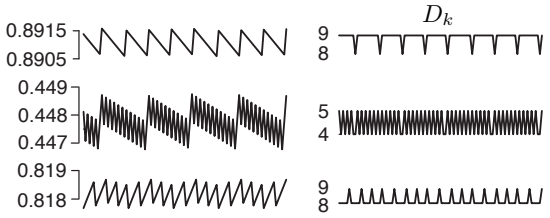

Fig. 7. Menagerie of oscillation figures obtained by simulating system (2) with various values (arbitrary units).

The period of the oscillations can nevertheless be arbitrarily long and the slightest imperfections or noise in the system can, in certain cases, cause it to switch from one regime to another. Such analysis could be approached by the study of peak-to-peak dynamics but the full analysis of these oscillations and of their possibly chaotic character is beyond the scope of this article.

As commented, oscillations in electromechanical systems with differentiation in the feedback arise in practice when the gain is high enough. This occurrence is easy to explain following the fact that the movements of such systems are often impeded by dry friction, however small, present whenever two surfaces in contact undergo relative movement. Dry friction, f_C, added to (2) can extinguish or prevent oscillations whenever

$$f_C > \frac{e}{B\nu},$$

in which case the state of the system can be constant from (2),(6) since the steady-state velocity can be zero.

As a final comment, it is possible to relate the system under study to the oversampling analog-to-digital converter or sigma-delta converter that operates on the principle of feeding the difference of time-shifted quantized outputs back to an integrator [4]. Such systems have been studied mostly through stochastic approaches since the objective is noise-reduction. A direct approach, as employed here, may also prove to be useful to study these systems.

Acknowledgements

The work was funded by a grant "High Fidelity Surgical Simulation" from the Natural Sciences and Engineering Council of Canada (NSERC).

6 Appendix

Proof of Theorem 2 The noise-free system,

$$m\,\dot{v}(t) + b\,v(t) = e(t) - B\nu\left(\lfloor\sigma_k\rfloor - \lfloor\sigma_{k-1}\rfloor\right), \quad (15)$$

$\forall k \in \mathbb{N}, t \in [kh, (k+1)h)$, is assumed to be at rest for times prior to zero, i.e. $x(t) = 0, \dot{x}(t) = 0, \forall t < 0$ the class of admissible forcing inputs is limited to $L_\infty([0,\infty))$. The solution to (15) is computed in a piecewise manner. It is easily verified that, for all $t \in [kh, kh+h)$, and for all $k \in \mathbb{N}$,

$$\begin{aligned} x(t) &= \kappa\nu d_k(t-hk) + x_k \\ &\quad - (-\kappa\nu d_k - \dot{x}_k)\,\tau_v(1-\alpha(t)) + g_1(t), \\ v(t) &= -\kappa\nu d_k(1-\alpha(t)) + v_k\alpha(t) + g_2(t), \\ g_1(t) &\triangleq \frac{1}{m}\int_0^t \int_{kh}^{kh+s} \alpha(\tau)e(\tau)d\tau ds, \\ g_2(t) &\triangleq \frac{1}{m}\int_{kh}^{kh+t} \alpha(\tau)e(\tau)d\tau. \end{aligned} \quad (16)$$

Let the sampled values of the state and velocity x_k and v_k at points $t = kh$ be defined in terms of left limits. Defining $z_k \triangleq \sigma_k - \sigma_{k-1}$ and introducing the quantization error, $\eta_k \triangleq \lfloor \sigma_k \rfloor - \sigma_k$,allows one to write the discretized solution (16) in the re-arranged form,

$$\begin{pmatrix} z_{k+1} \\ v_{k+1} \end{pmatrix} = \Phi \begin{pmatrix} z_k \\ v_k \end{pmatrix} + \begin{pmatrix} F_1 \\ F_2 \end{pmatrix} + \begin{pmatrix} \delta_{1k} \\ \delta_{2k} \end{pmatrix}, \tag{17}$$

$$\Phi \triangleq \begin{pmatrix} -\kappa\left(1 - \xi\tau_n(1-\alpha_h)\right) & \rho\tau_n(1-\alpha_h) \\ -\kappa\nu(1-\alpha_h) & \alpha_h \end{pmatrix}, \tag{18}$$

$$F_1 \triangleq \rho g_1(h) = \rho \int_0^h g_2(s)ds, \quad F_2 = g_2(h), \tag{19}$$

$$\delta_{1k} \triangleq -\kappa\left(1 - \xi\tau_n(1-\alpha_h)\right)(\eta_k - \eta_{k-1}), \tag{20}$$

$$\delta_{2k} \triangleq -\kappa\nu(1-\alpha_h)(\eta_k - \eta_{k-1}). \tag{21}$$

Inputs F_1 and F_2 are uniformly bounded as follows

$$\begin{aligned} |F_1| = \rho|g_1(h)| &\leq \rho\frac{e_k}{m}\int_0^h \int_{kh}^{kh+s} e^{(\varsigma - kh)/\tau_n} d\varsigma ds \\ &\leq \frac{e_k}{b\nu}(1 - \xi\tau_n(1-\alpha_h)) \\ |F_2| = |g_2(h)| &\leq \frac{e_k}{m}\int_{hk}^{hk+h} e^{(\varsigma - kh)/\tau_n} d\varsigma \\ &\leq \frac{e_k}{b}(1-\alpha_h). \end{aligned}$$

where $e_k \triangleq \operatorname{ess\,sup}_{k=0,\infty}\{e(t); t \in [kh, (k+1)h)\}$. It is convenient to write (17) with a piecewise constant input defined by $\{e_k\}_{k=0}^{\infty}$,

$$\begin{pmatrix} z_{k+1} \\ \dot{x}_{k+1} \end{pmatrix} = \Phi \begin{pmatrix} z_k \\ \dot{x}_k \end{pmatrix} + \Gamma_1 e_k - \Gamma_2(\eta_k - \eta_{k-1}), \tag{22}$$

where,

$$\Gamma_1 = \frac{1}{b}\begin{pmatrix} \nu^{-1}\left(1 - \xi\tau_n(1-\alpha_h)\right) \\ (1-\alpha_h) \end{pmatrix},$$

$$\Gamma_2 = \kappa\begin{pmatrix} \left(1 - \xi\tau_n(1-\alpha_h)\right) \\ \nu(1-\alpha_h) \end{pmatrix}.$$

It is noticed that the control transformation

$$e_k = u_k - B\nu(\eta_k - \eta_{k-1}), \tag{23}$$

brings (22) into a system without quantization drift,

$$\begin{pmatrix} z_{k+1} \\ \dot{x}_{k+1} \end{pmatrix} = \Phi \begin{pmatrix} z_k \\ \dot{x}_k \end{pmatrix} + \Gamma_1 u_k. \tag{24}$$

Since the quantization error sequence is bounded, the BIBO stability of (22) is equivalent to the BIBO stability of (24). If the discretization (15) into (24) is non-pathological in that the sampling period is selected to ensure that the controllability of (17), (22), and (24) is preserved and the pair $[\Phi, \Gamma_1]$ is controllable.

It follows that (24) is L_∞-BIBO stable from the input e_k if and only if $r(\Phi) < 1$, with $r(\Phi) \triangleq \max_{i=1,2}\{|\lambda_i(\Phi)|\}$, the spectral radius of matrix Φ [5]. The L_∞-BIBO stability of the system in continuous time follows from the stability of the discretized system (is in fact equivalent) when $x_k = x(kh), v_k = v(hk)$, $\forall k \in \mathbb{N}$. The application of the Bellman-Gronwall Lemma delivers a bound for the state of the system in between discretization instants. Specifically, there exists a constant K such that $|x(t)| \leq K|x(kh)|, |v(t)| = K|v(hk)|$, $\forall t \in [kh, (k+1)h)$, $k \in \mathbb{N}$.

An explicit bound for the trajectories of (22) can then be derived. The solution of (22) and, specifically, its velocity component, is obtained by using the variation of constants formula,

$$\begin{aligned} v_k = C\begin{pmatrix} z_k \\ \dot{x}_k \end{pmatrix} &= C\Phi^{k-1}\begin{pmatrix} z_1 \\ v_1 \end{pmatrix} + \sum_{l=1}^{k-1} C\Phi^{k-l-1}\Gamma_1 e_l \\ &\quad - \sum_{l=1}^{k-1} C\Phi^{k-l-1}\Gamma_2(\eta_l - \eta_{l-1}) \\ &= C\Phi^{k-1}\begin{pmatrix} z_1 \\ \dot{x}_1 \end{pmatrix} + \sum_{l=1}^{k-1} C\Phi^{l-1}\Gamma_1 e_{k-l} \\ &\quad - \sum_{l=1}^{k-1} C\Phi^{l-1}\Gamma_2(\eta_{k-l} - \eta_{k-l-1}). \end{aligned}$$

For large k, the effect of the initial condition decays to zero, and restricting to a constant input, e, yields the bound for the discretized velocity,

$$\begin{aligned} \|\{v_k\}_{k=1}^{\infty}\|_\infty &\leq O(k) + |e|\left\|\sum_{l=1}^{\infty} C\Phi^{l-1}\Gamma_1\right\|_\infty \\ &\quad + \left\|\sum_{l=1}^{\infty} C\Phi^{l-1}\Gamma_2(\eta_{k-l} - \eta_{k-l-1})\right\|_\infty \\ &\leq |e|\left|C(I-\Phi)^{-1}\Gamma_1\right| \\ &\quad + \|\{\eta_{l+1} - \eta_l\}_{l=0}^{\infty}\|_\infty \left\|\left\{C\Phi^l\Gamma_2\right\}_{l=0}^{\infty}\right\|_1 \end{aligned} \tag{25}$$

where $O(k)$ represents a discrete-time function such that $O(k) \to 0$ as $k \to \infty$, because for any $\{a_n\}_{n=0}^{\infty} \in l_1$ and $\{b_n\}_{n=0}^{\infty} \in l_\infty$, $\|\sum_{n=0}^{\infty} a_n b_n\|_\infty \leq \|\{a_n\}\|_1 \|\{b_n\}\|_\infty$. In view of the sum of the von Neumann series $\sum_{l=1}^{\infty} C\Phi^{l-1}\Gamma_1 = C(I-\Phi)^{-1}\Gamma_1$ which is valid if $r(\Phi) < 1$. The effect of the initial condition is captured by $O(k)$, as claimed. □

References

[1] J. J. Abbott and A. M. Okamura. Effects of position quantization and sampling rate on virtual wall passivity. *IEEE Transactions on Robotics*, 21(5):952–964, 2005.

[2] K. H. Ang, G. Chong, and Y. Li. PID control system analysis, design, and technology. *IEEE Transactions on Control Systems Technology*, 13(4):559–576, 2005.

[3] P. Belanger, P. Dobrovolny, A. Helmy, and X. Zhang. Estimation of angular velocity and acceleration from shaft-encoder measurements. *The International Journal of Robotics Research*, 11(1225–1230), 1998.

[4] J. C. Candy. *Delta-Sigma Data Converters: Theory, Design, and Simulation*, chapter An overview of basic concepts, pages 1–43. Wiley-IEEE-Press, 1996.

[5] T. Chen and B. Francis. *Optimal Sampled-data Control Systems*. Springer Verlag, 1995.

[6] J. E. Colgate and G. Schenkel. Passivity of a class of sampled-data systems: Application to haptic interfaces. In *Proceedings of the American Control Conference*, pages 3236–3240, 1994.

[7] D. F. Delchamps. Stabilizing a linear system with quantized state feedback. *IEEE Transactions On Automatic Control*, 35(8):916–924, 1990.

[8] N. Diolaiti, G. Niemeyer, F. Barbagli, and K. Salisbury. Stability of Haptic Rendering: Quantization, Discretization, Time-Delay and Coulomb Effects. *IEEE Transactions on Robotics and Automation*, 18(1):1–10, 2006.

[9] A. H. Gosline and V. Hayward. Eddy current brakes for haptic interfaces: Design, identification, and control. *IEEE/ASME Transactions on Mechatronics*, 13(6):669–677, 2008.

[10] R. M. Gray and T. G. Stockham. Dithered quantizers. *IEEE Transactions On Information Theory*, 39(3):805–812, 1993.

[11] J. P. Hespanha, P. Naghshtabrizi, and Y. Xu. A survey of recent results in networked control systems. *Proceedings of the IEEE*, 95(1):138–182, 2007.

[12] F. Janabi-Sharifi, V. Hayward, and C.-S. J. Chen. Discrete-time adaptive windowing for velocity estimation. *IEEE Transactions On Control Systems Technology*, 8(6):1003–1009, 2000.

[13] R. C. Kavanagh and J. M. D. Murphy. The effects of quantization noise and sensor nonideality on digital differentiator-based rate measurement. *IEEE Transactions On Instrumentation And Measurement*, 47(6):1457–1463, 1998.

[14] L. H. Keel, J. I. Rego, and S. P. Bhattacharyya. A new approach to digital pid controller design. *IEEE Transactions On Automatic Control*, 48(4):687–692, 2003.

[15] E. Kofman. Quantized-state control: a method for discrete event control of continuous systems. *Latin Am. Appl. Res.*, 33(4):399–406, 2003.

[16] S.-H. Lee, T. A. Lasky, and S. A. Velinsky. Improved velocity estimation for low-speed and transient regimes using low-resolution encoders. *IEEE/ASME Transactions on Mechatronics*, 9(3):553–560, 2004.

[17] M. Lemkin, P. H. Yang, A. C. Huang, and D. M. Auslander. Velocity estimation from widely spaced encoder pulses. In *Proceedings of the American Control Conference*, pages 998–1002, 1995.

[18] D. Liberzon. Hybrid feedback stabilization of systems with quantized signals. *Automatica*, 39:1543–1554, 2003.

[19] H. Michalska and V. Hayward. Quantized and sampled control of linear second order systems. In *Proceedings of the European Control Conference 2009*, pages 531–536, 2009.

[20] T. Petrila and D. Trif. *Basics of Fluid Mechanics and Introduction to Computational Fluid Dynamics*, pages 259–264. Springer Science and Business Media, 2005.

[21] M. R. Sirouspour, S. P. DiMaio, S. E. Salcudean., P. Abolmaesumi, and C. Jones. Haptic interface control-design issues and experiments with a planar device. In *Proceedings of IEEE International Conference on Robotics and Automation*, volume 1, pages 789–794, 2000.

[22] Y. Su, C. Zheng, P. Mueller, and B. Duan. A simple improved velocity estimation for low-speed regions based on position measurements only. *IEEE Transactions on Control Systems Technology*, 14(5):937—942, 2006.

[23] E. E. Wallingford and J. D. Wilson. High-resolution shaft speed measurements using a microcomputer. *IEEE Transactions On Instrumentation And Measurement*, 26(2):113–116, 1977.

[24] B. Widrow. Statistical analysis of amplitude-quantized sampled-data systems. *Applications and Industry*, pages 1–14, 1961.